



Relationships of surface ozone with its precursors, particulate matter and meteorology over Delhi

Ashima Sharma^{1,2} · T. K. Mandal^{1,2}  ·
S. K. Sharma^{1,2} · D. K. Shukla¹ · S. Singh^{1,2}

Received: 8 March 2016 / Accepted: 1 November 2016 /
Published online: 22 November 2016
© Springer Science+Business Media Dordrecht 2016

Abstract The paper presents the temporal variations of surface ozone (O_3) and its precursors (oxides of nitrogen (NO_x), carbon monoxide (CO), methane (CH_4) and non-methane hydrocarbons (NMHCs)) along with particulate matter (PM_{10} and $PM_{2.5}$) and their relationship with meteorology during January 2012 to December 2014 at an urban site of Delhi, India. The mean mixing ratio of surface O_3 , NO_x , CO, CH_4 and NMHCs were 29.5 ± 7.3 ppb, 34.7 ± 11.2 ppb, 1.82 ± 0.52 ppm, 3.07 ± 0.37 ppm and 0.53 ± 0.17 ppm, respectively. This study also comprises an analysis of the relation between UV irradiance and surface O_3 . A relationship between the total oxidant concentrations (OX) and NO_x has been used to identify the regional background O_3 values and the local levels of primary pollution. An attempt has been made to identify the existence of NO_x or NMHC sensitive regime by charting out relationships between O_3 , NO_x and NMHCs. The respective high pollution periods of surface O_3 and PM differ on a seasonal timescale. Linear regression analysis has been used to quantify the negative influence of the chemical constituents of PM (elemental carbon, NO_3^- , SO_4^{2-}) on O_3 values. Statistical validation using bivariate correlation analysis, multiple linear regression (MLR) analysis and principal component analysis (PCA) strongly describes the intricate relationships among the aforesaid variables and meteorology. Potential Source Contribution Function (PSCF) and Concentration Weighted Trajectory (CWT) analysis indicated upper Indo-Gangetic Plain (IGP) as a significant source region of O_3 precursor gases contributing for O_3 values at the study site.

Electronic supplementary material The online version of this article (doi:10.1007/s10874-016-9351-7) contains supplementary material, which is available to authorized users.

✉ T. K. Mandal
tuhin@nplindia.org

¹ Environmental and Biomedical Metrology Division, CSIR-National Physical Laboratory, Dr KS Krishnan Road, New Delhi -110012, India

² Academy of Scientific and Innovative Research (AcSIR), CSIR-National Physical Laboratory Campus, Dr. K S Krishnan Road, New Delhi -110012, India

Keywords Ozone · NO_x · NMHCs · Particulate matter · Meteorology · UV irradiance · PSCF · CWT

1 Introduction

Atmospheric trace gases, despite their relative scarcity, subsist as chemically reactive factors influencing the thermal budget, atmospheric chemistry, ecology and human health (Ramanathan et al. 1985) whereas particulate matter (PM), has been shown to be linked with cardiovascular mortality (Pope et al. 2004), respiratory morbidity (Schwartz 1993) and detrimental health effects (Chow et al. 2006; Pope et al. 2009), more so in biologically susceptible populations (Chow and Watson 2006; R uckerl et al. 2011; Sacks et al. 2011) as well as affecting the atmospheric photochemistry.

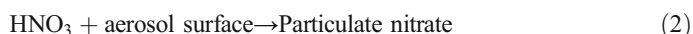
Tropospheric ozone (O₃) (Tilton 1989) is a secondary product of the oxidation of hydrocarbons (CH₄ and NMHCs) and CO via reactions catalyzed by HO_x and NO_x radicals (Crutzen 1995; Jacob 2000) (Fig. 1). While NO_x primarily regulates the oxidizing capacity of the atmosphere through partitioning or formation of free radical species (OH, HO₂ and RO₂), CO and CH₄-NMHCs serve as a sink for the reactive OH radicals (Wayne et al. 1991). As a greenhouse gas, O₃ contributes to global warming (Staehelin et al. 2001; Hansen et al. 2005) exerting prominent impacts on environment, health and vegetation (Delfino et al. 1998; Finlayson-Pitts and Pitts 1999; Weschler 2006). It is also a strong oxidizing agent and a vital source of OH radical (Chameides and Walker 1973; Thompson 1992) accountable for major chemical transformations in the atmosphere (Crutzen and Zimmermann 1991), especially in the tropics, making it the photochemically most active region in the world (Naja and Lal 2002). Inevitably, India is at a reasonably higher risk, alongside a grim apprehension that this pollution will further extend from a local to global scale. Besides, South-East Asia is an anthropogenically active zone and model calculations have anticipated a potential for considerable environmental impacts owing to increasing surface O₃ values, exclusively in India, China etc. (Berntsen et al. 1996) and NASA/GISS calculations have shown that the O₃ production efficiency (OPE) is greatest over the Indian subcontinent (Saini et al. 2014). This validates a need for the continuous monitoring of atmospheric trace gases and their secondary by-products.

Several studies have hence been conducted around the globe during the past three decades showing presence of a clear seasonal cycle of surface O₃ over the continents. Winter maximum was observed at many remote/ rural locations (Logan 1985; Ayers et al. 1997; Gros et al. 1998; Monks 2000; Varotsos et al. 2002) whereas spring/ summer maximum have also been reported (Oltmans and Levy 1992; Derwent et al. 1998; Pochanart et al. 1999). Likewise in India, various groups have carried out surface O₃ measurements in different regions (Varshney and Aggarwal 1992; Jain and Arya 2001; Nair et al. 2002; Jain et al. 2005; Ghude et al. 2006; Mittal et al. 2007; Ghude et al. 2008; Mahapatra et al. 2012; Ojha et al. 2012; Sharma et al. 2013; Peshin et al. 2014; Sharma et al. 2016a) and their observations elucidating the regional air quality have been very useful.

Besides the trace gases, PM is an additional significant tropospheric component comprising both fine (PM_{2.5}) and coarse (PM₁₀) fractions (Pope and Dockery 2006). Source apportionment studies have confirmed diverse sources of PM (Sharma et al. 2014; Sharma et al. 2016b) which are integrated into the particulate phase by different

processes. PM affects the atmospheric photochemistry by its ability to scatter the solar and terrestrial radiation, indirectly altering the air temperature and subsequently affecting chemical rate coefficients. The same has been established by model simulations that have calculated a reduction in the O₃ mixing ratios as an effect of these UV-absorbing aerosols (Dickerson et al. 1997). It is hence desirable to comprehend the gas phase-aerosol interactions that serve as the sink of O₃ precursors to condense upon (Bauer et al. 2007), dissolve within or react on their surfaces (Jacobson 1998).

The reactive chemical species are transferred to aerosols with vapor molecules initially diffusing to their surface, eventually reacting with other soluble and reactive species. The sorption of a gas onto a particle is a two body (vapor and particle) chemical reaction (reaction 1) and its rate coefficient depends on the number density of particles, the size of the particle, the nature of the diffusing species and other factors. Studies have documented this process; the alkalinity of mineral dust (Schütz and Sebert 1987) supports the uptake of gaseous species; the presence of transition metals such as Fe and Mn in the Asian dust offers reaction surfaces for soluble species such as OH, HO₂ and H₂O₂ (Gao et al. 1992); the heterogeneous oxidation of nearly 60% of the tropospheric SO₂ to SO₄²⁻ has also been credited to aerosols (Luria and Sievering 1991). Moreover, atmospheric NO_x (or N₂O₅) sinks on the surfaces of mineral aerosols as nitrate and eventually yields nitric acid (HNO₃) which is a termination reaction in the photochemical O₃ system, implying that the production rate of HNO₃ is a function of ambient values of NO_x and OH. These denitrification processes (reaction 2, 3) leading to formation of particulate nitrate are expected to lower the ambient air levels of NO_x (Rodriguez et al. 1991) subsequently influencing the O₃ chemistry (Zhang et al. 1994) and it is desirable to compute the magnitude of this influence.



Along with the pollutant emissions in the lower atmosphere, air pollution also depends on the favorable meteorological conditions with meteorology playing a critical function in transport, formation or accumulation of trace species within the atmospheric boundary layer (ABL) (Kleinman et al. 1994; Toh et al. 2013; Ma et al. 2016). Hence, an assessment of its behavior with O₃ values is obligatory to figure out the observed trends and to analyze the controlling nature of meteorology concerning pollution levels in the city.

The key objective of this study is to elucidate the temporal variations and interrelationships of surface O₃ and its precursors, oxides of nitrogen (NO_x), carbon monoxide (CO), methane (CH₄) and non-methane hydrocarbons (NMHCs) along with particulate matter (PM₁₀ and PM_{2.5}) and meteorology. Present analysis of combined data set (O₃ precursor gases, UV irradiance and meteorology) which are required to generate and/or influence surface O₃ provides a conclusive study for an urban site.

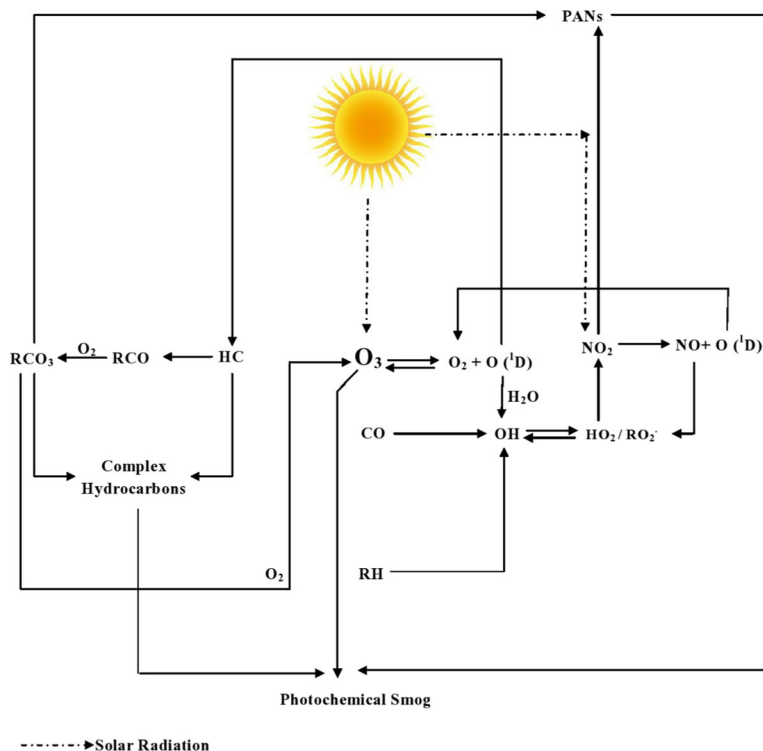


Fig. 1 The details of O_3 chemistry: Atmospheric oxidation efficiency is largely determined by OH radicals. Photodissociation of O_3 by solar UV radiation produces electronically excited $O(^1D)$ atoms which combine with water vapor to produce OH radicals. Reaction with OH is the major atmospheric sink for most trace gases and the primary precursor pollutants (CO and hydrocarbons (HCs)) react with OH to produce hydroperoxyl (HO_2) or organic peroxy (RO_2) radicals, respectively. These radicals react with NO (produced from photodissociation of NO_2) to generate more NO_2 and OH radicals, at the same time as the $O(^1D)$ atoms can either oxidize to produce O_3 or in presence of HCs, react together to produce acyl (RCO) radicals which get oxidized to form peroxyacyl (RCO_3) radicals. The RCO_3 radicals can react with more HCs to produce complex organic species of aldehydes and ketones, or it can react with NO_2 to produce peroxyacyl-nitrate (PANs) or get oxidized to produce O_3 and inevitably generate the ingredients of photochemical smog

2 Methodology

2.1 Description of site

The sampling location at CSIR-National Physical Laboratory (CSIR-NPL), New Delhi ($28^{\circ}38' N$, $77^{\circ}10'E$; 216 m amsl) represents a typical urban atmosphere, surrounded by huge roadside traffic and agricultural fields in the southwest direction (Fig. 2). Delhi experiences highly variable weather throughout the three major seasons- scorching summers (March–June) followed by humid monsoons (July–October) and cold winters (November–February). Intense heat, low humidity and dust laden hot winds from the west bound Thar Desert are a conspicuous feature of Delhi's summer. The start of rainy season is marked by the advent of moisture laden south-western winds, traveling from the Arabian Sea. The average annual rainfall in the city is ~ 617 mm. Chilly north-western winds from the Himalayas are accountable for the winter onset. This shift in the wind pattern also provides access to the polluted air

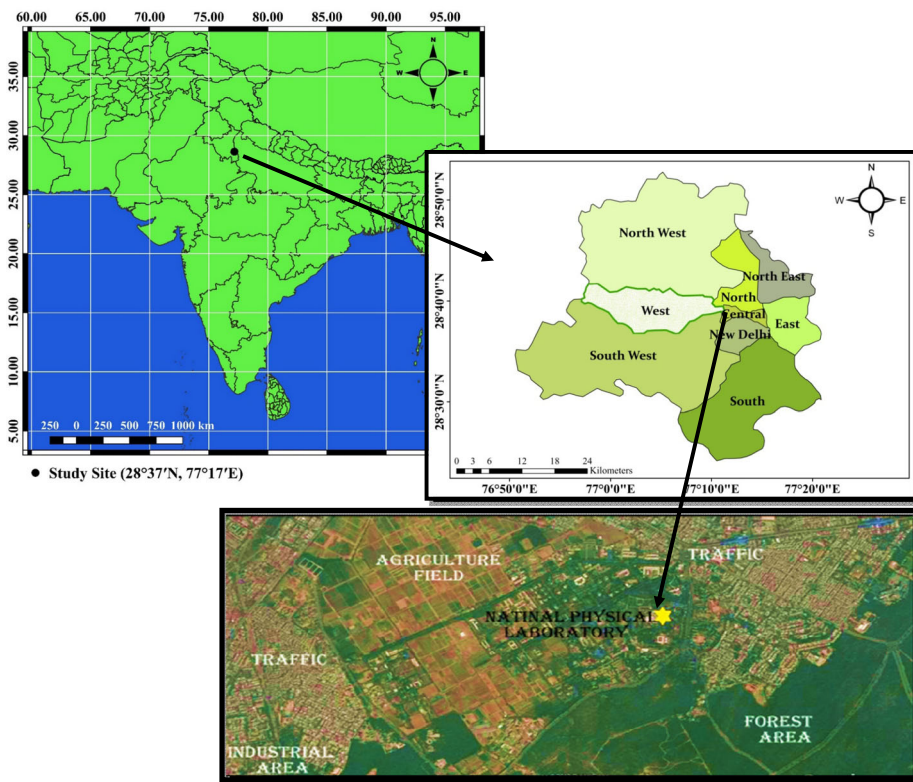


Fig. 2 The study site (CSIR-National Physical Laboratory) at New Delhi, India ($28^{\circ}37'N$, $77^{\circ}17'E$; 216 m amsl)

masses along with fog and poor visibility. High variations between summer and winter temperatures is a characteristic trait of Delhi's climate. As an urban site with intense anthropogenic activities and fluctuating weather patterns, it provides for a suitable location to study the active chemistry of surface O_3 and its precursors.

2.2 Experimental setup

The measurements of trace gases (O_3 , NO_x , CO, CH_4 and NMHCs), PM_{10} and $PM_{2.5}$ samples and the meteorological parameters (temperature (Temp), relative humidity (RH), wind speed (WS), wind direction (WD), UV irradiance) were carried out during January 2012 to December 2014 with the help of ground based analyzers, particulate samplers and automatic weather station (AWS), respectively.

A UV-based O_3 analyzer (Model 49C; M/s The Thermo Environmental Instruments Inc.) was used for measurement of surface O_3 (accuracy ± 1 ppb). The O_3 analyzer was calibrated periodically with the Primary Ozone Standard of CSIR-NPL, New Delhi (Standard Reference Photometer) with an accuracy of $< \pm 2\%$. NO and NO_2 were measured using NO_x -Analyzer (Model CLD 88 p; M/s ECO Physics AG.) using a photocatalytic converter (Model: PLC 866; M/s ECO Physics AG.) with an accuracy of ± 0.05 ppb. NO_x analyzer was calibrated periodically using Pure Air Generator (Model: PAG 003; M/s ECO Physics AG, accuracy 0.01 ppb) and NIST-USA certified NO gas (500 ppb $\pm 5\%$). CO was measured using non-

dispersive infrared (NDIR) gas filter correlation analyzer (Model 48C; M/s Thermo Environmental Instruments Inc.). CO analyzer was calibrated periodically using Pure Air Generator and NIST-USA certified CO gas ($8.1 \text{ ppm} \pm 5\%$) with multi gas calibrator. CH₄ and NMHCs were measured using flame ionization detection (FID) based hydrocarbon analyzer (Model APHA-360; M/s Horiba) and their measurements were conducted for a period of nine months (April–December 2014). Zero and span gas of hydrocarbon analyzer were calibrated using Pure Air Generator and NIST-USA certified CH₄ gas ($8.0 \text{ ppm} \pm 5\%$). These analyzers were operated continuously (20–25 days in each month) during the measurement period with an uninterrupted power supply. The inlets of all the analyzers were stationed at ~10 m height (above the ground). The mixing ratios of these gases were recorded at a 1 min time resolution and computed on an hourly basis. The other details of these analyzers including their working principles etc. are summarized in supplementary information S1.

PM₁₀ and PM_{2.5} samples were collected simultaneously on Whatmann quartz microfiber (QM-A) filters which were initially pre-baked at 550°C in a muffle furnace for at least 5 h to eliminate all impurities and then kept in a desiccator for a period of 24 h prior to sample collection which was done using the particle samplers (APM 550, Make: M/s. Envirotech, India; one unit for PM₁₀ and another unit for PM_{2.5}). Ambient air was passed through a 47 mm diameter QM-A filter at a flow rate of $1 \text{ m}^3 \text{ h}^{-1}$ (accuracy $\pm 2\%$) for 24 h during the sampling period. The flow meter of the samplers was calibrated (with the accuracy of $\pm 2\%$ of Full Scale) with air flow calibrator traceable to national standard. The concentrations of PM₁₀ and PM_{2.5} (in $\mu\text{g m}^{-3}$) were calculated on the basis of the difference between final and initial weights of the quartz filters measured by a micro balance (M/s. Sartorius, resolution $\pm 10 \mu\text{g}$) and dividing the difference by the total volume of air passed during the sampling. After collecting samples, filters were stored under dry conditions at -20°C in the deep-freezer. Analysis of elemental carbon (EC) and ionic components (NO_3^- and SO_4^{2-}) have been carried by an OC/EC carbon analyzer (Model: DRI 2001A, USA; Make: Atmoslytic Inc., USA) and Ion Chromatograph (Model: DIONEX-ICS-3000, USA) with conductivity detector, respectively. Details of OC-EC and ion analysis are described in Sharma et al. (2015).

In addition, the meteorological parameters (Temp, RH, WS, WD) were measured by a five-stage meteorological tower (30 m height), installed in the same campus, about 100 m away from the observational site. We made use of the meteorological data accessible at level 2 (10 m height). The solar flux measurements for total UV (direct + diffuse) have been done using a radiometer (Model: CUV-4; Make: Kipp and Zonen). The instrument is intended to measure irradiance resulting from radiant fluxes incident upon a plane surface from the hemisphere above in the bandwidth 280–400 nm. The radiant flux measurements of CUV-4 has experimental errors $<10\%$ in the total flux during the day. The flux data (in Wm^{-2}) were obtained every 2 min, 24 h a day during the entire observation period.

2.3 Analysis methods

For analysis of a three year data-set, the first approach involved investigating the time series and comprehensively probing the temporal variations of the measured parameters using frequently used statistical methods and graphical representations. This was followed by the application of Pearson correlation test, Multiple Linear Regression (MLR) analysis and Principal Component Analysis (PCA) to identify the relationships amongst the observed atmospheric variables. This supported a detailed evaluation of our collected dataset. Source identification for surface O₃ was executed utilizing the data for isentropic 1-day backward

trajectories. Isentropic backward trajectories were selected since they replicate a more realistic motion of air parcels allowing for their displacement (vertical motions) in an adiabatic atmosphere (Harris and Kahl 1990; Oltmans et al. 1996). Subsequent to this, we used GIS based tools (Potential Source Contribution Function and Concentrated Weighted Trajectory analysis) for statistical examination of the trajectories in collaboration with the O₃ measurements to derive results.

3 Results and discussion

3.1 Temporal variations of the trace gases

Annual mean of O₃ mixing ratio was calculated to be 26.1 ± 7.5 ppb, 25.8 ± 4.3 ppb and 36.6 ± 10.0 ppb during 2012, 2013 and 2014, respectively. Annual mean of NO_x and CO mixing ratios were recorded to be 34.3 ± 9.1 ppb, 30.6 ± 12.6 ppb, 39.4 ± 11.9 ppb and 1.67 ± 0.68 ppm, 1.93 ± 0.45 ppm, 1.85 ± 0.43 ppm during 2012, 2013 and 2014, respectively. The mean mixing ratio of CH₄ and NMHCs during the measurement period was recorded to be 3.07 ± 0.37 ppm and 0.53 ± 0.17 ppm, respectively. Figure 3 shows box and whisker plots illustrating the average monthly variations of the gases and as a measure of variability for individual months, the mean, median, 25th and 75th percentiles and the maximum–minimum values were plotted. For surface O₃, the statistical mean was greater than the median for all months, excluding July and August, suggesting that the outliers (high values) are towards the upper end of the distribution, signifying high O₃ values, except in the monsoon months. For CO, NO_x and CH₄, the majority of the mean values were roughly equivalent to the median value, which signifies an approximately symmetric distribution. The time series of the trace gases, surface O₃, NO_x, CO, CH₄ and NMHCs, presenting the arrangement of data (Bisht et al. 2015) is given in Fig.S1 (in supplementary information). It shows the temporal evolution of the daily mean measurements of the various parameters. A 10 day moving average of the daily mean values is made to smoothen out the fluctuations in the collected data. There exists a noteworthy daily, monthly and seasonal variability for all the measured parameters. Surface O₃ shows high value during the month of May. Beginning from June, following the summer season, the mixing ratio for surface O₃ reaches its lowest levels for at least two months. The month of October appears to be the time when the pollutant concentrations start hiking up after a relatively cleaner monsoonal hiatus. Table S1 (in supplementary information) summarizes the monthly average values of the variables, calculated by using hourly averages of the measured data.

To determine the seasonal–diurnal trends of the trace gases during the measurement period, the observed data was initially grouped on the basis of the three major seasons, winter (November–February), summer (March–June) and monsoon (July–October) and then plotted against time (Fig. S2; in supplementary information). Seasonal variations for trace gases are mainly influenced by difference in convection processes, photochemical removal, source strengths etc. (Jobson et al. 1994; Klonecki et al. 2003). The O₃ mixing ratio at this site demonstrates typical diurnal cycles with maxima during afternoon [12:00–14:00 h IST–(Indian Standard Time)] and minima in the early morning hours (05:00–07:00 h) and the late night hours (00:00–02:00 h) (Nair et al. 2002; Naja et al. 2003; Jain et al. 2005; Sharma et al. 2016b). Evidently, the diurnal profile during the monsoons depicted a shorter climb on account of a relatively cleaner atmosphere.

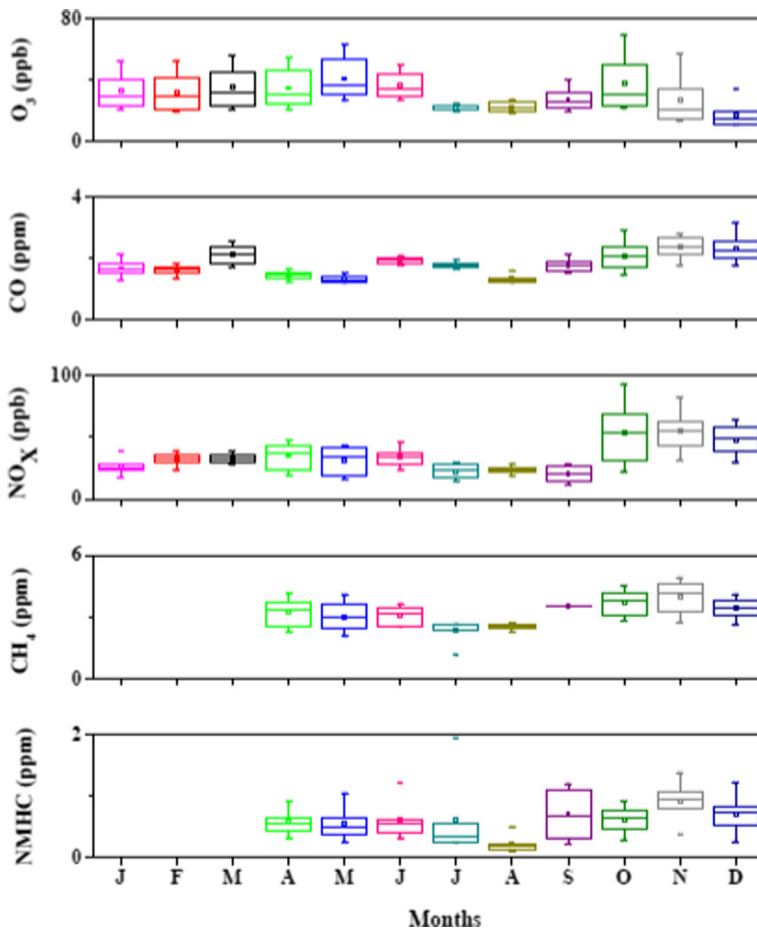


Fig. 3 Statistical analysis of O_3 , CO, NO_x , CH_4 and NMHCs at the study site (the horizontal solid line indicates the median, the square indicates the mean, top and bottom of the box indicate the 75th and 25th percentile, respectively, top and bottom crosses in the whiskers indicate the maximum and minimum values, respectively)

Unlike O_3 , the average diurnal cycle of the precursor gases show noticeably patterns (Ahmed et al. 2006; Beig et al. 2007; Purkait et al. 2009). The prominent diurnal profiles of CO are dual-peaked (Pun et al. 2003), one during the early morning hours (07:00–08:00 h) and the second during night (20:00–21:00 h). The CO minimum is observed during afternoon, usually around 15:00 h, because of a high mixing layer (Chow et al. 1999). Since CO is an O_3 precursor, its reducing values indicates that it helps in maintaining O_3 build up in presence of sunlight even after peak hours. The dual peaked behavior is particularly prominent during the winter months. This should be credited to the incomplete combustion of hydrocarbons in vehicular fuel (Chinkin et al. 2003; Parrish 2006) coupled with low boundary layer height owing to low temperatures triggering peaked behavior during the traffic hours. Similarly, the diurnal profile of NO_x show minima in the afternoon hours, during the time O_3 begins to show a buildup, suggesting its part in photochemical conversion (Bhugwant and Brémaud 2001) while the maximum is observed during night and early morning hours, possibly due to increased vehicular emissions due to traffic hours, given that NO_x is an indicator of fossil

fuel based emissions (Vellingiri et al. 2015; Sharma et al. 2016a). Related diurnal profiles are recorded for both CH₄ and NMHCs indicating their role as a surface O₃ precursor. CH₄ shows buildup during early morning hours possibly because the study site is near to the agricultural fields of the Indian Agricultural Research Institute (IARI), New Delhi (Neue et al. 1997; Mosier et al. 1998) and its recognized that the biological processes control the exchange of CH₄ (Nishanth et al. 2014). The peaks are also discernible during the evening traffic hours (20:00–21:00 h) and that is likely as the hydrocarbons are released into the ambient air due to partial or negligible burning of hydrocarbon based vehicular fuels. Clear seasonal variability was identified for CH₄ and NMHCs with distinct maxima during winters. Similar set of observations have been witnessed in different studies across the world (Dueñas et al. 2002; Tu et al. 2007).

The average surface O₃ values during daytime (06:00–17:00 h) and nighttime (18:00–05:00 h) for the measurement period (Table S2; in supplementary information) were used to estimate the average rate of increase of O₃, calculated to be 1.12 ppb h⁻¹. Similar observations at other sites show different results; Anantapur (1 ppb h⁻¹; Reddy et al. 2008), Kannur (1.3 ppb h⁻¹; Nishanth 2012) and Kullu (2.4 ppb h⁻¹; Sharma et al. 2013). The maximum and minimum O₃ values observed during individual months have also been given in Table S2 (in supplementary information). We used the data to calculate the ratio, O_{3max}/O_{3min} which has been proposed to be a pollution indicator (Saliba et al. 2008); for urban and highly polluted sites, the values are reported in excess of 10 (Cvitas et al. 1995) while lower values have been reported for relatively cleaner areas. O_{3max}/O_{3min} of the order of 22.9 indicates the study location is an urban, polluted site. Another distinct feature of an urban polluted site is a sharp daytime increase in surface O₃ value and to assess that, the rate of change of O₃ was calculated between 08:00–12:00 h and 17:00–21:00 h (Table S3; in supplementary information) and found to be 5.25 ppb h⁻¹ and -3.55 ppb h⁻¹, respectively. Since the rate of decrease is far less than the rate of increase, O₃ values are increasing. The diurnal rate of change of O₃(dO₃/dt) for different seasons was calculated and the results have been summarized in Table S4 and Fig. S3 (in supplementary information). The rate of change was highest during the winter season primarily due to the related meteorological conditions. Additionally, sharp changes during 09:00–10:00 h and 16:00–18:00 h for all seasons indicates the influence of increased emission of precursor gases, especially from vehicles during traffic hours and the associated meteorology as well to O₃ titration. Also, the dry deposition process of O₃ on surfaces of leaves or soil leads to its loss (Chameides and Walker 1973; Wesely and Hicks 2000).

3.2 Relationship of O₃ with particulate matter (PM₁₀ and PM_{2.5})

The preceding section elucidates that trace gas pollution at the study site is increasing. Besides the trace gases, high levels of PM is also an indicator of a deteriorating air quality. It has been observed that PM exhibits highest concentrations during the winter months of November to February (Fig. S4; in supplementary information). Monthly average PM_{2.5} concentrations during the measurement period ranged between 34.9 ± 20.4 μgm⁻³ (September) to 270.2 ± 98.7 μgm⁻³ (January) while for PM₁₀, it ranged between 76.7 ± 27.6 μgm⁻³ (September) to 367.1 ± 154.4 μgm⁻³ (December). Higher PM concentrations during winters and higher O₃ values during summers justifies a need for a separate study of O₃ and PM on the grounds that their respective high pollution periods are not concurrent on seasonal timescales but on a diurnal scale, both of them are sensitive to boundary layer variations and meteorology, however only weakly negatively correlated (Table 1). Yet, PM and O₃ are known to share a

Table 1 Correlation matrix of O₃ with PM₁₀ and PM_{2.5} concentrations and with their individual components (EC, NO₃⁻ and SO₄²⁻)

Parameters	<i>R</i>	Regression equation
O ₃ versus PM ₁₀	0.23	O ₃ = -0.02 PM ₁₀ + 37.85
O ₃ versus EC	0.37	O ₃ = -0.45 EC (PM ₁₀) + 40.57
O ₃ versus NO ₃ ⁻	0.49	O ₃ = -0.49 NO ₃ ⁻ (PM ₁₀) + 37.61
O ₃ versus SO ₄ ²⁻	0.29	O ₃ = -0.37 SO ₄ ²⁻ (PM ₁₀) + 37.59
O ₃ versus PM _{2.5}	0.27	O ₃ = -0.04 PM _{2.5} + 36.54
O ₃ versus EC	0.21	O ₃ = -0.32 EC (PM _{2.5}) + 35.25
O ₃ versus NO ₃ ⁻	0.28	O ₃ = -0.38 NO ₃ ⁻ (PM _{2.5}) + 36.81
O ₃ versus SO ₄ ²⁻	0.24	O ₃ = -0.54 SO ₄ ²⁻ (PM _{2.5}) + 35.92

chemical coupling (Meng et al. 1997) but unanswered questions linger concerning the possible effects of PM on the photochemical oxidant cycle and eventually on O₃.

The primary organic particulate emissions incorporate in the PM as the black (elemental) carbon core coated by organic material (Mauderly and Chow 2008) and might reduce O₃ by 5–8% (Penner et al. 1993) by absorbing solar and terrestrial radiation or as an ingredient of the CCN (Jensen and Toon 1997). In a study by Li et al. 2005, black carbon aerosol reduced the photolysis frequencies, *J* [O₃(¹D)] and *J* [NO₂] in the ABL. To validate this, we correlated PM_{2.5} and PM₁₀ and their common chemical constituents such as EC, NO₃⁻ and SO₄²⁻ with O₃ and obtained weak negative correlations (Table 1). Following this, simple linear regression analysis was executed to predict O₃ values based on the concentrations of EC, NO₃⁻ and SO₄²⁻. The regression equation obtained was used to quantify the influence of these chemical constituents of PM on O₃. It was found out that the EC component of PM_{2.5} and PM₁₀ decreased the O₃ values by 9.7% and 16.6%, respectively. Similarly, the NO₃⁻ component of PM_{2.5} and PM₁₀ decreased O₃ values by 13.4% and 16.9%, respectively while the SO₄²⁻ component did the same by 23.9% and 17.8%, thus confirming our proposition.

3.3 Relationship of O₃ with UV irradiance

Figure 4a represents a column plot between O₃ and UV irradiance using their integrated averages to assess the relationship between them. It is evident that UV irradiance begins to take effect around 06:00 h reaching highest value at noon around 12:00 h and its peak coincides with the highest O₃ values. This advocates the central role of solar UV flux in O₃ production. Both parameters demonstrate a similar diurnal trend, but while UV irradiance begins to plunge after 13:00 h, O₃ continues to show high values till 17:00 h. This is due to the persistent release and occurrence of precursor gases, reacting and eventually generating O₃. The mean UV irradiance was found to be highest during summers (16.39 Wm⁻²) followed by monsoon (14.51 Wm⁻²) and winter (12.27 Wm⁻²). The hourly averaged UV irradiance values range between <1 Wm⁻² to 48.36 Wm⁻² during the measurement period. The hourly mean values (06:00–17:00 h) have been calculated for each month followed by average on a seasonal basis (Fig. 4b). It explains the seasonal-diurnal classification of the relation between surface O₃ and UV irradiance. It can be observed that high O₃ values during summers and monsoon exist for a longer duration between 8:00–15:00 h. During winters, due to higher PM concentration,

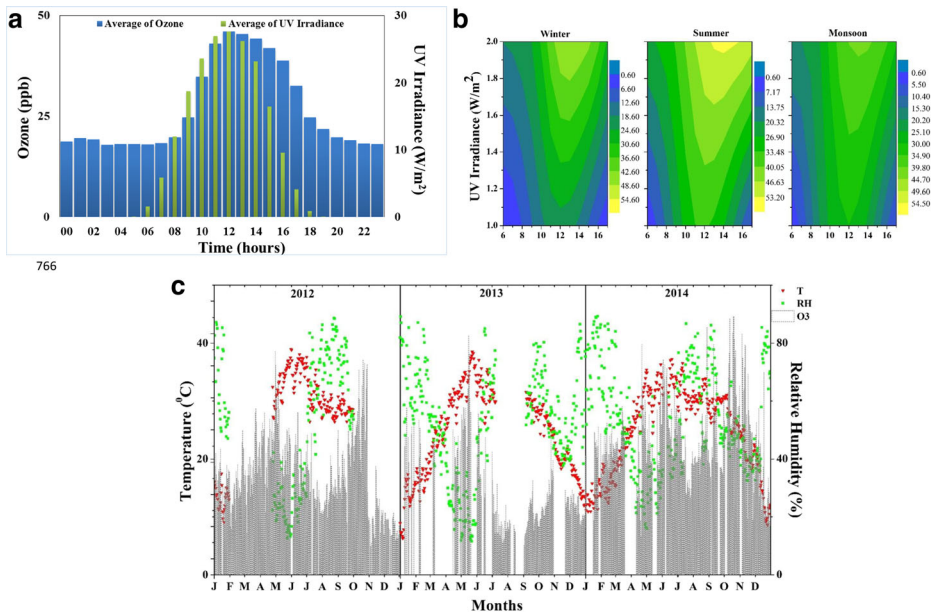


Fig. 4 a Average relationship between O₃ and UV irradiance with respect to time b Contour plots depicting seasonal relationships between O₃ and UV irradiance c Relationship between Temperature, Relative Humidity and O₃

absorption and scattering of the radiation is expected (Bano et al. 2013). Correlation analysis was attempted between O₃ and UV irradiance; summer ($r = 0.47$), winter ($r = 0.53$) and monsoon ($r = 0.38$).

3.4 Relationship of O₃ with meteorology

Table 2 describes the average mixing ratio of trace gases determined within selected ranges of temperature. The relationship between O₃ and temperature is indirect (Fig. 4c), executing itself through higher downward solar radiation. As O₃ production is a photochemical reaction involving radicals, high temperature promotes this rate of reaction, the propagation of the radical chains and inevitably O₃ formation (Tu et al. 2007; Martins et al. 2012). On the contrary, the O₃ precursors show high values within low temperature ranges, probably since low temperatures prohibit their convective dispersal, resulting in their buildup in the ABL. Surface O₃ and RH are inversely related; the highest RH values are observed during monsoons when ambient air O₃ values are the lowest (Fig. 4c). Likewise, the diurnal pattern of RH indicates elevated levels at midnight and

Table 2 Average mixing ratio of trace gases determined within selected ranges of temperature

Temperature ranges (°C)	O ₃ (ppb)	NO _x (ppb)	CO (ppm)	CH ₄ (ppm)	NMHCs (ppm)
≥10 - ≤20	26.38	35.87	1.87	3.41	0.71
>20 - ≤30	29.42	36.61	1.85	3.39	0.60
>30	32.20	29.47	1.69	2.81	0.55

in the early morning, gradually dipping after sunrise contrary to the diurnal profile of O_3 . This might occur due to loss of O_3 due to water vapor (Fig. 1).

Wind allows the dispersal of the trace pollutant species along horizontal and vertical levels by promoting the mixing and transport across/ in-between the boundary layer and the upper free atmosphere. The plot relating the diurnal profiles of O_3 and WS in Fig. 5a signifies that high WS are accountable for the transboundary transport of O_3 laden air. High wind speeds during the afternoon are accompanied by higher O_3 mixing ratios and low wind speeds during early morning and late night contribute to the O_3 sinking process. Also, high WS removes PM and increases the incoming solar radiation and thus boosts O_3 formation (Zhang et al. 2015). Figure 5b represents contour plots relating the diurnal and seasonal profiles of WS and WD. It is evident that high wind speeds within the range of $1.4\text{--}2.2\text{ ms}^{-1}$ are a distinguishable feature of summers (which record the highest O_3 mixing ratio). This suggests that winds transport pollutant laden gases to the study site and the prevailing meteorological conditions support O_3 formation. However, in winters, the low wind speeds within the range of $0.6\text{--}1\text{ ms}^{-1}$ during early morning and late night hours complement the relatively lower O_3 . Moreover, wind direction (WD) delivers an understanding of the first order advection process and correlating the surface O_3 data with WD provides insight into the impact of air mass transport on surface O_3 variability (Lin et al. 2008). Specific WD's are found to influence air pollutants more than other directions since the emission intensities of pollutants in those directions are comparatively higher because of regional transport (Zhang et al. 2015). Figure 5c shows that the specific directions with lower wind speeds support the accumulation of air pollutants and also the average O_3 in different wind direction sectors segregated seasonally and it can be observed that the highest values appear in the ESE- SW sectors. A probable reason can be the presence of two coal based thermal power plants (Badarpur and Faridabad) located in this sector, a few kilometers distant from the study site and contribute to the regional transport of pollutant loaded air in the direction of the study site.

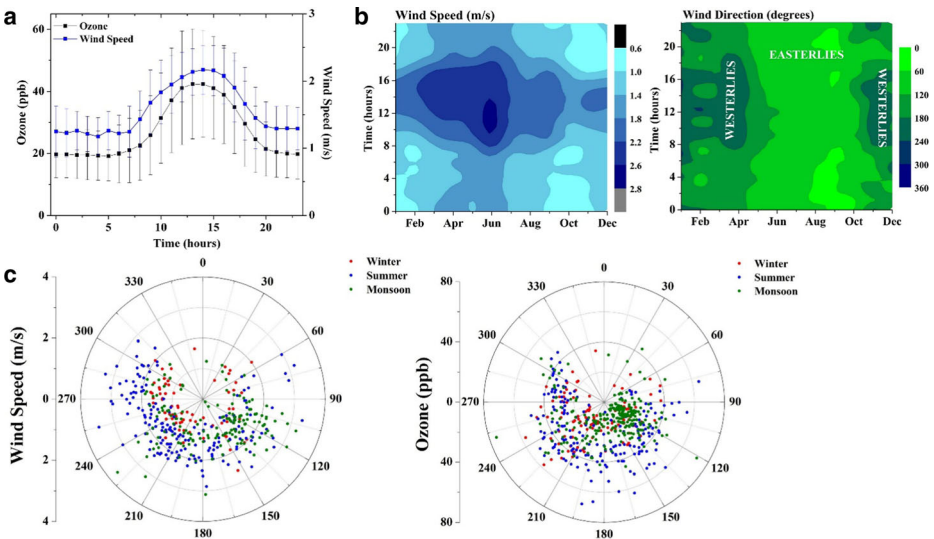


Fig. 5 a Average diurnal profiles of surface O_3 and WS during the observational period at the study site. The error bars indicate one standard deviation b Contour plots demonstrating the diurnal and monthly variation of WS and WD c Bivariate polar plots depicting relationship between WS-WD and O_3 -WD

3.5 Statistical analysis

To describe the complex relationships between O_3 and the many variables that may cause or hinder its production, we first analyzed whether our data was normally distributed so as to understand whether to apply a parametric or a non-parametric correlation test (S2; in supplementary information). We eventually employed a parametric test (Pearson Correlation Test) to understand the relationship between the quantitative variables. An additional advantage of correlation analysis is that study of parameters with different units is achievable using this method (Özbay et al. 2011). Table 3 presents the correlation values among all variables. As observed, O_3 negatively correlated with CO, $PM_{2.5}$ and RH. Amongst these, RH was most strongly correlated and displayed a significant correlation, $r(12) = -0.585$ (at $p \leq 0.05$). Surface O_3 positively correlated with NO_x , CH_4 , NMHCs, PM_{10} , Temp, WS, WD and UV irradiance. Strong positive relationships were observed between the O_3 precursors, CH_4 and NO_x , $r(12) = 0.759$ and NMHCs and NO_x , $r(12) = 0.567$ signifying their interactions in the troposphere, with hydrocarbons oxidizing to produce O_3 in reactions catalyzed by NO_x (Fig. 1). A strong correlation coefficient (0.892) between CH_4 and NMHCs proposes that these locally emitted pollutants have a key role in active photochemistry (Nishanth et al. 2014). As discussed before, UV irradiance and WS is negatively correlated with PM_{10} and $PM_{2.5}$, validating that PM scatters and absorbs radiation while high WS removes PM. Temperature and UV irradiance share strong significant correlation, $r(12) = 0.873$. The results are compatible with the available literature (Abdul-Wahab et al. 2005; Yerramsetti et al. 2013).

Multiple Linear Regression (MLR) analysis was also implemented to find out the relationship between surface O_3 and the explanatory variables (precursors) (S3 in supplementary information). We obtained the following equation,

$$[O_3] = 36.04 - 1.38[NO_x] - 13.82[CO] + 44.94[CH_4] - 21.50[NMHCs] \\ + 0.04[PM_{10}] + 0.01[PM_{2.5}] + 1.31[T] - 0.68[RH] - 29.85[WS] - 0.08[WD]$$

A multiple correlation coefficient (R) is the measure of the strength of the relationship between the dependent variable and the ten independent variables selected for inclusion in the equation. In this study, $R = 0.998$ was observed, suggesting an extremely strong linear relationship. By squaring 'R', we identified the value of the coefficient of multiple determinations (i.e. R^2). This statistic enables us to determine the amount of explained variation (variance) in Y (O_3) from the ten predictors on a range of 0–100% (Ilten and Selici 2008). Thus we are able to say that 99.64% of variation in $[O_3]$ was accounted for through the combined linear effects of the predictor variables and that approximately 99.6% points fall on the regression line and fit the model. Another statistic (adjusted R^2 value) compares the explanatory power of regression models, unaffected by the number of predictor variables (Dominick et al. 2012). It was calculated to be 0.960.

Principal Component Analysis (PCA) is a dimension reduction technique for restructuring the data where the output is essentially measured by correlation (Yong and Pearce 2013). This technique is useful in this study because it extracts maximum variance from the data set and thus reduces a large number of variables into smaller number of uncorrelated components, thereby facilitating an identification of the most dominant groups of pollutants and meteorological parameters. PCA was applied by using the monthly averaged data for the variables (O_3 ,

Table 3 Correlations between input variables

	Ozone	NO _x	CO	CH ₄	NMHCs	PM ₁₀	PM _{2.5}	T	RH	WS	WD	Irradiance
Ozone	1											
NO _x	0.077	1										
CO	-0.027	0.084	1									
CH ₄	0.185	0.759*	-0.043	1								
NMHCs	0.034	0.567	-0.241	0.892*	1							
PM ₁₀	0.061	0.574	-0.399	0.725*	0.783*	1						
PM _{2.5}	-0.214	0.441	-0.281	0.688*	0.733*	0.769*	1					
T	0.276	-0.313	0.249	-0.724*	-0.820*	-0.771*	-0.826*	1				
RH	-0.585*	-0.330	0.035	-0.037	-0.060	-0.055	0.241	-0.447	1			
WS	0.303	-0.477	-0.430	-0.602*	-0.453	-0.405	-0.525	0.649*	-0.508	1		
WD	0.468	0.522	-0.069	0.690*	0.699*	0.428	0.489	-0.278	-0.524	-0.101	1	
Irradiance	0.359	-0.540	0.005	-0.766*	-0.713*	-0.673*	-0.870*	0.873*	-0.476	0.837*	-0.302	1

*Correlation is significant at the $p < 0.05$ level

NO_x, CO, CH₄, NMHCs, PM₁₀, PM_{2.5}, Temp, RH, WS and WD) over the measurement period using SPSS software. The Kaiser-Meyer-Olkin (KMO) statistic was used to measure the suitability of the factor analysis (Supplementary information S4); the value was 0.622 and so we were confident of the application of factor analysis on our data set. Additionally, for factor analysis to work, we need a significant Bartlett's test (significance value $p < 0.05$), so as to justify existence of some relationship between the input variables. The results indicated that the test was highly significant ($p < 0.001$) and therefore, factor analysis was appropriate.

In this study, the principle components (PCs) were extracted based on Eigen value (greater than 1) as rest are not significant (Kim et al. 2009) and the eleven initial variables were decreased (extracted) to three PCs. While the first PC accounts for an approximately 32% of the total variance, the cumulative contribution of the three PCs is about 73% variability (Table S5; supplementary information). Each PC corresponds to the collective behavior of the original variables and the Eigen values associated with each variable depicts the amount of variance depicted by that linear component. For a better interpretation, factors are rotated; Varimax rotation, a type of orthogonal rotation has been used because it minimizes the number of variables that have high loadings on each factor and works to make small loadings even smaller (Statheropoulos et al. 1998) (Table 4). The output of the component matrix before rotation contains the loadings of each variable onto each factor but since all loadings less than 0.3 were to be suppressed in the output and so there are blank spaces for many of the loadings. The rotated component matrix is the key output of PCA and contains estimates of the correlations between each of the variables and the estimated components. Through PCA, the concentrations of the meteorological parameters were grouped to PC1, the values of O₃ and its precursor gases (NO_x, CH₄, NMHC) were grouped to PC2 while PC3 corresponds to the concentrations of PM (PM₁₀ and PM_{2.5}). Strong correlations have been witnessed between the traffic related pollutants (CO and NO_x) in PC1. A strong correlation of NO_x with other pollutants was identified in PC2 which is an indication of a collective influence of urban landscape including the traffic movement, local topography, atmospheric chemistry and physical processes (Beckerman et al. 2008).

Table 4 PCA resolved component matrix after Varimax rotation

	Component		
	PC1	PC2	PC3
Ozone		0.667	
NO _x	-0.677	0.484	
CO	-0.568		0.341
CH ₄		0.903	
NMHC		0.880	
PM ₁₀		0.404	0.730
PM _{2.5}			0.923
Temp	0.847		
RH	0.677		0.417
WS	0.898		
WD	0.771		0.371

We have also calculated correlations between O_3 , NO_x and CO with UV irradiance during different times of the day to find out the role of dominant parameters in determining O_3 production during the day (06:00–17:00 h). The analysis period has been subdivided into 3 time zones based on the variation in the diurnal trends of the trace gases: 06:00–08:00 h (early morning), 11:00–13:00 h (midday) and 15:00–17:00 h (late day hours) (Table 5). It can be observed that O_3 is strongly correlated with UV irradiance (0.58) during early morning hours. NO_x is strongly negatively correlated with O_3 during complete day length, signifying the critical role of NO_x in O_3 production at the study site. Like NO_x , CO also shows strong negative correlations with O_3 during early morning hours indicating that photochemical activity of O_3 begins during morning hours due to precursor availability (i.e., NO_x and CO). During midday when O_3 reaches peak values, correlations between O_3 and UV irradiance are moderate (0.30), but, less as compared to morning hours. As expected CO shows insignificant correlation with O_3 (−0.15) diminishing its direct role in formation of O_3 , however, NO_x sustain the O_3 buildup even after peak hours. The reported wavelength of UV dataset in the present study is in the range of 280–400 nm. The equivalent wavelength for the dissociation energy of NO_2 is ~390.3 nm and hence NO_x shows weak negative correlation with UV irradiance during early morning hours but is strongly negatively correlated with UV irradiance during the noon time, suggesting that it photochemically converts to O_3 . The results establish that oxidation of CO with OH to produce peroxy radicals is more significant in O_3 chemistry than its relationship with UV irradiance.

Moreover, we have attempted to establish how the oxidant concentrations ($[OX] = O_3 + NO_2$) vary with the level of NO_x . This allows us to understand the variability and behavior of oxidant levels, which depend on numerous factors such as photochemical reactions, convective mixing of pollutants, long range transport or the height of the ABL (Notario et al. 2013). The slope of the relationship between $[OX]$ and $[NO_x]$ (Fig. 6a) show the local OX contributions, while the intercept is suggestive of the NO_x independent regional contribution (Varotsos et al. 2014). The regression lines of the $[OX]$ vs. $[NO_x]$ was:

$$[OX] = 0.562 [NO_x] + 8.293 \text{ with, } r = 0.66$$

This basically suggests that the NO_x independent regional contribution which is essentially equivalent to the background O_3 value is relatively low than the local contribution which is a linear function of the local emissions and largely dependent on the primary pollution. The variation of $[NO_2] / [OX]$ with $[NO_x]$ was plotted in Fig. 6b to determine the proportion of $[OX]$ in the form of NO_2 and an analysis of the plot

Table 5 Correlations between the different parameters during different time of the day

Time (h)	UVI vs. O_3	UVI vs. NO_x	UVI vs. CO	O_3 vs. NO_x	O_3 vs. CO
06:00–08:00	0.58	-0.14	-0.08	-0.63	-0.54
11:00–13:00	0.30	-0.44	-0.15	-0.62	-0.15
15:00–17:00	0.41	-0.38	-0.21	-0.64	-0.13

UVI: UV irradiance

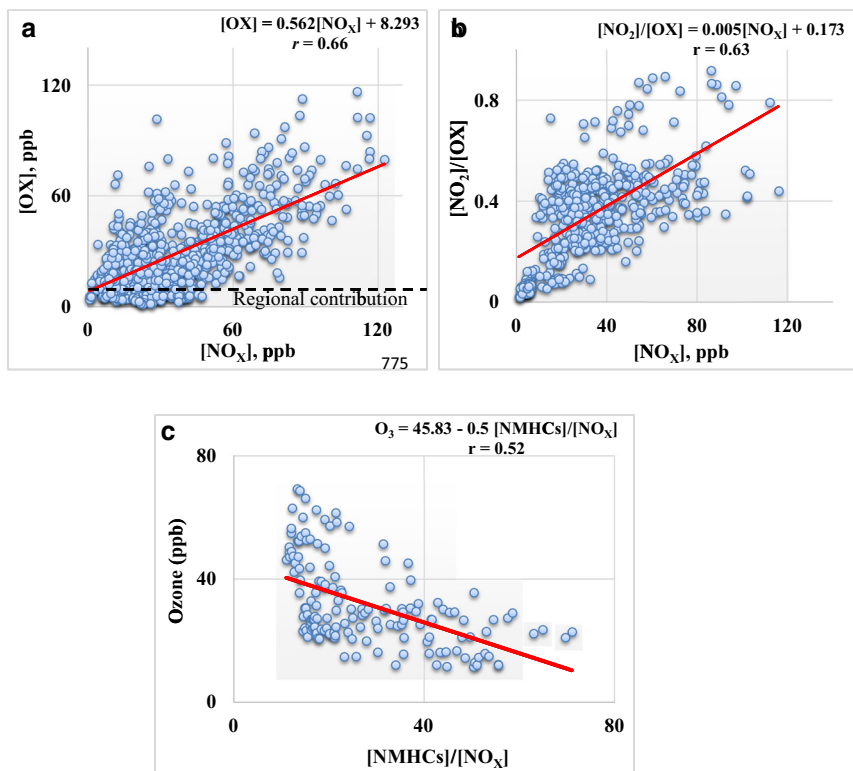


Fig. 6 Variation of a) $[\text{NO}_x]$ vs. $[\text{OX}]$ b) $[\text{NO}_x]$ vs. $[\text{NO}_2]/[\text{OX}]$ c) $[\text{O}_3]$ vs. $[\text{NMHCs}]/[\text{NO}_x]$

reveals a linear relationship with the increase in the levels of the ratio $[\text{NO}_2] / [\text{OX}]$ with increasing levels of NO_x suggesting that a major proportion of OX is present in the form of NO_2 . The regression lines of the $[\text{NO}_2] / [\text{OX}]$ vs. $[\text{NO}_x]$ was:

$$[\text{NO}_2]/[\text{OX}] = 0.005 [\text{NO}_x] + 0.173 \text{ with, } r = 0.63$$

We can infer that a major proportion of oxidants at the study site are in the form of NO_2 and that relative to the background surface O_3 values, the local emissions of primary pollutants are high in the ambient air of the city. Moreover, $[\text{NMHCs}]/[\text{NO}_x]$ ratio was calculated to recognize the role of NO_x in generation or inhibition of O_3 . High $[\text{NMHCs}]/[\text{NO}_x]$ ratio (24.57) was observed which suggests that there exists a NO_x sensitive regime at the study site, letting NO_x to cater to the role of an O_3 generator. This ratio differs for a location and for time of day; during nighttime hours, it was nearly two times (35.28) the ratio observed during daytime hours (17.63). Since, NMHCs do not have any secondary sources in the atmosphere and simply the emission processes near the source regions contribute to their abundance, it can be concluded that vehicular emissions, solvent evaporation, industrial releases etc. during nighttime along with the boundary layer processes are accountable for the high nighttime ratio. A scatter plot showing correlation between $[\text{O}_3]$ and $[\text{NMHCs}]/[\text{NO}_x]$ (Fig. 6c) demonstrates an inversely proportional relationship between the two parameters, validating that O_3

increases with increasing NO_x (NO_x sensitive). Due to possible emission of particular species of NMHCs, the regime changes of O_3 dependency on NO_x is quite important.

3.6 Analysis of air mass back trajectories

One day backward isentropic air mass trajectories were computed using the NOAA (National Oceanic and Atmospheric Administration) Air Resource Laboratory (ARL) Hybrid Single Particle Lagrangian Integrated Trajectory (HYSPLIT) model with the Global Data Assimilation System (GDAS) data (<http://www.arl.noaa.gov>) as an input. The trajectories were calculated at 500 m above ground level (AGL) for the sampling duration and have been represented in Fig. 7a. They have been plotted in order to show the origin of the air masses and their transport pathways to the sampling site and it is apparent that they originate from the continental land masses to reach the receptor site and so allow an influx of gaseous and particulate pollutants. These groups of trajectories have been clustered together (Fig. 7b) to represent the major directions of the air mass offering a better conception of the source regions. Cluster analysis splits the ‘n’ number of trajectories into distinct groups (clusters) based on the transport speed and direction, eventually yielding clusters with similar length and curvature (Brankov et al. 1998; Li et al. 2012). To chart the source potentials of the studied geographical region to facilitate identification of the probable source regions contributing to elevated levels of O_3 , a potential source contribution function (PSCF) analysis was done (Fig. 7c) using air mass trajectories statistics software, TrajStat (version 1.2.2.6). PSCF is the ratio of polluted trajectory segment endpoints falling in a grid cell to the total number of trajectory endpoints passing over that grid (Wang et al. 2009). The PSCF value can be interpreted as the conditional probability that an air parcel which passed through a grid cell during transport to the receptor

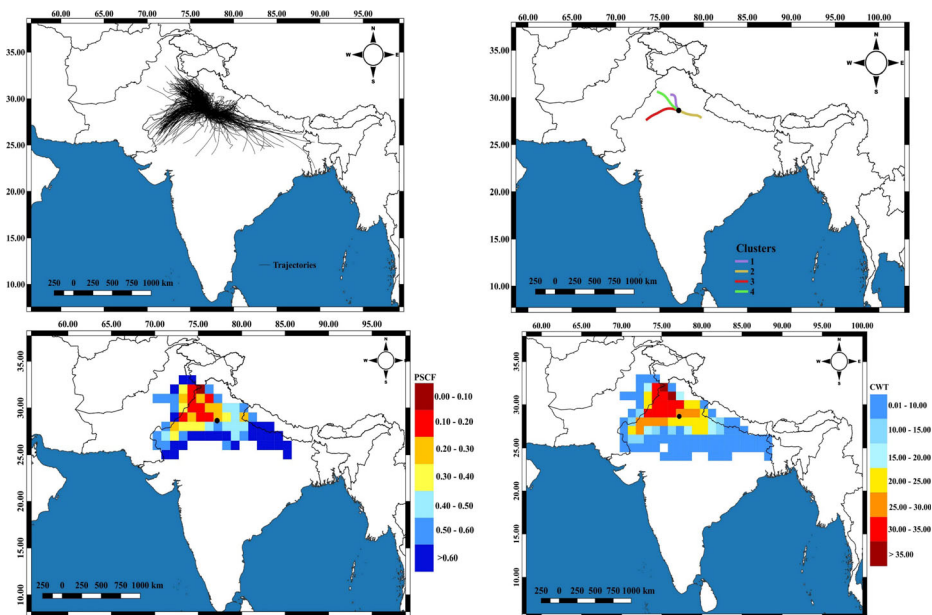


Fig. 7 a Five day back trajectories b Clustered Trajectory Analysis c PSCF Analysis d) CWT Analysis of surface O_3 during January 2012 – December 2014. The black circle represents the study site at New Delhi

site had a high concentration upon arrival at the trajectory endpoint (Hopke 2003). The color coding is used to denote the lowest to highest probability grids (in our study, the 60th percentile of O₃ mixing ratio was used as the pollution criterion value) to identify cells containing emission sources. The probable source grids span the densely populated and polluted regions of Northern India, spanning the Indo-Gangetic Plain (IGP) including parts of Haryana, Punjab, Rajasthan, Uttar Pradesh as well as parts of Pakistan which contain key oil fields, refineries and major thermal power plants (Naja et al. 2014). Thus, the air masses flowing from these regions are bound to bring pollutant laden gases to the receptor site and in due course generate secondary pollutants such as surface O₃. Nonetheless, PSCF method has a problem in distinguishing between strong and moderate sources. Even though it identifies the potential source areas, it is unable to allocate their discrete contribution to the measured concentrations at the receptor site and so the concentration weighted trajectory (CWT) model is used to help define the relative significance of potential sources. In CWT, every concentration is used as a weighting factor for the residence times of all trajectories in each grid cell and then divided by the cumulative residence time from all trajectories (Cheng et al. 2013). CWT analysis also points out the contribution of the IGP towards pollution at the receptor site (Fig. 7d). The strongest contributors remain parts of Punjab followed by Rajasthan, Haryana and Uttar Pradesh. It is known that these regions are greatly urbanized and highly populated and boast of numerous thermal power plants for energy generation. Moreover, the enormous amounts of burning of agricultural crop residues in these fertile farmlands is a critical issue (Jain et al. 2014) that has also been adjudged a contributing factor (Badarinath et al. 2009) to the high values of gaseous and particulate emissions.

4 Conclusion

The study takes account of the measurements of trace gases (O₃, NO_x, CO, CH₄, NMHCs), particulate matter (PM_{2.5} and PM₁₀) and meteorological parameters (Temp, RH, WS, WD, UV irradiance) during the period of January 2012 to December 2014. Following are the prominent outcomes of the study:

- Over the 3 years measurement period, the mean mixing ratio of surface O₃, NO_x, CO, CH₄ and NMHCs were calculated to be 29.5 ± 7.3 ppb, 34.7 ± 11.2 ppb, 1.82 ± 0.52 ppm, 3.07 ± 0.37 ppm and 0.53 ± 0.17 ppm, respectively. Their temporal evolution displayed notable variability revealing high values. The pollution indicator ratio (O_{3max}/O_{3min}) exhibited high value (22.9), confirming high O₃ pollution at the study site. The O₃ production was observed to occur at a rate of 1.12 ppb h⁻¹.
- The study recognizes that a separate analysis of O₃ and PM on a seasonal timescale is ideal given the difference in their high pollution periods. Linear regression analysis was used to interpret the influence of the chemical constituents (EC, NO₃⁻ and SO₄²⁻) of PM (both fine and coarse fractions) on surface O₃ values, revealing negative effects.
- UV irradiance shows strong positive correlation with O₃, temperature and WS and strong negative correlations with PM validating its role in O₃ generation, and verifies that PM scatters or absorbs radiation. Both the mean UV irradiance and O₃ mixing ratio were found to be highest during summers. But, UV irradiance recorded lowest values during the winter season implying the role of other factors and meteorology in determining O₃ levels.

- An evaluation of the role of meteorology on the mixing ratio of O₃ verifies that pollution at the study site is an amalgamation of two factors: high emissions of precursor gases and meteorological factors encouraging the formation and buildup of secondary pollutants.
- Bivariate correlation analysis, MLR analysis and PCA were implemented on the data set to corroborate the observed relationships and the results supported our findings. It was also found out that a major proportion of the total oxidant concentration [OX] at the study site is in the form of NO₂ and local emissions of primary pollutants are high in comparison to the regional background O₃ value. High [NMHCs]/[NO_x] ratio denote NO_x sensitive conditions implying that NO_x serves to be an O₃ generator at the study site. Strong correlation of NO_x with other variables during different daytime period implies the influential role of NO_x in O₃ formation. Backward trajectory, PSCF and CWT analysis established that the major source regions for O₃ pollution are located in and around the city.

Acknowledgments Authors are thankful to the Director, CSIR-National Physical Laboratory (NPL), New Delhi and Head, Environmental and Biomedical Metrology Division, CSIR-NPL, New Delhi, India for their constant encouragement and support. Authors thankfully acknowledge the ISRO-GBP, Ahmedabad for financial support under the AT-CTM program (GAP-114732). The authors would like to thank Dr. S.R. Radhakrishnan, Scientist, CSIR-NPL, New Delhi for providing meteorological datasets. One of the authors (AS) thanks the University Grants Commission (UGC), New Delhi for awarding the Junior Research Fellowship (JRF). The authors are thankful to the anonymous reviewers for their constructive suggestions to improve the manuscript.

References

- Abdul-Wahab, S.A., Bakheit, C.S., Al-Alawi, S.M.: Principal component and multiple regression analysis in modelling of ground-level ozone and factors affecting its concentrations. *Environ. Model Softw.* **20**(10), 1263–1271 (2005)
- Ahammed, Y.N., Reddy, R.R., Gopal, K.R., Narasimhulu, K., Basha, D.B., Reddy, L.S.S., Rao, T.V.R.: Seasonal variation of the surface ozone and its precursor gases during 2001–2003, measured at Anantapur (14.62 N), a semi-arid site in India. *Atmospheric Research.* **80**(2), 151–164 (2006)
- Ayers, G.P., Granek, H., Boers, R.: Ozone in the marine boundary layer at cape grim: model simulation. *J. Atmos. Chem.* **27**(2), 179–195 (1997)
- Badarinath, K.V.S., Kharol, S.K., Sharma, A.R.: Long-range transport of aerosols from agriculture crop residue burning in indo-Gangetic Plains—a study using LIDAR, ground measurements and satellite data. *J. Atmos. Sol. Terr. Phys.* **71**(1), 112–120 (2009)
- Bano, T., Singh, S., Gupta, N.C., John, T.: Solar global ultraviolet and broadband global radiant fluxes and their relationships with aerosol optical depth at New Delhi. *Int. J. Climatol.* **33**(6), 1551–1562 (2013)
- Bauer, S.E., Koch, D., Unger, N., Metzger, S.M., Shindell, D.T., Streets, D.G.: Nitrate aerosols today and in 2030: a global simulation including aerosols and tropospheric ozone. *Atmos. Chem. Phys.* **7**(19), 5043–5059 (2007)
- Beckerman, B., Jerrett, M., Brook, J.R., Verma, D.K., Arain, M.A., Finkelstein, M.M.: Correlation of nitrogen dioxide with other traffic pollutants near a major expressway. *Atmos. Environ.* **42**(2), 275–290 (2008)
- Beig, G., Gunthe, S., Jadhav, D.B.: Simultaneous measurements of ozone and its precursors on a diurnal scale at a semi urban site in India. *J. Atmos. Chem.* **57**(3), 239–253 (2007)
- Berntsen, T., Isaksen, I.S., Wang, W.C., Liang, X.Z.: Impacts of increased anthropogenic emissions in Asia on tropospheric ozone and climate. *Tellus B.* **48**(1), 13–32 (1996)
- Bhugwant, C., Brémaud, P.: Simultaneous measurements of black carbon, PM10, ozone and NO_x variability at a locally polluted island in the southern tropics. *Journal of atmospheric chemistry.* **39**(3), 261–280 (2001)
- Bisht, D.S., Dumka, U.C., Kaskaoutis, D.G., Pipal, A.S., Srivastava, A.K., Soni, V.K., Attri, S.D., Sateesh, M., Tiwari, S.: Carbonaceous aerosols and pollutants over Delhi urban environment: temporal evolution, source apportionment and radiative forcing. *Sci. Total Environ.* **521**, 431–445 (2015)
- Brankov, E., Rao, S.T., Porter, P.S.: A trajectory-clustering-correlation methodology for examining the long-range transport of air pollutants. *Atmos. Environ.* **32**(9), 1525–1534 (1998)

- Chameides, W., Walker, J.C.: A photochemical theory of tropospheric ozone. *J. Geophys. Res.* **78**(36), 8751–8760 (1973)
- Cheng, I., Zhang, L., Blanchard, P., Dalziel, J., Tordon, R.: Concentration-weighted trajectory approach to identifying potential sources of speciated atmospheric mercury at an urban coastal site in Nova Scotia, Canada. *Atmospheric Chemistry and Physics*. **13**(12), 6031–6048 (2013)
- Chinkin, L.R., Coe, D.L., Funk, T.H., Hafner, H.R., Roberts, P.T., Ryan, P.A., Lawson, D.R.: Weekday versus weekend activity patterns for ozone precursor emissions in California's south coast Air Basin. *Journal of the Air & Waste Management Association*. **53**(7), 829–843 (2003)
- Chow, J.C., Watson, J.G.: Overview of ultrafine particles and human health. *WIT Trans. Ecol. Environ.* **99**, 619–632 (2006)
- Chow, J.C., Watson, J.G., Lowenthal, D.H., Hackney, R., Magliano, K., Lehrman, D., Smith, T.: Temporal variations of PM_{2.5}, PM₁₀, and gaseous precursors during the 1995 integrated monitoring study in central California. *Journal of the Air & Waste Management Association*. **49**(9), 16–24 (1999)
- Chow, J.C., Watson, J.G., Mauderly, J.L., Costa, D.L., Wyzga, R.E., Vedal, S., Hidy, G.M., Altshuler, S.L., Marrack, D., Heuss, J.M., Wolff, G.T.: Health effects of fine particulate air pollution: lines that connect. *J. Air Waste Manag. Assoc.* **56**(10), 1368–1380 (2006)
- Crutzen, P.J.: Ozone in the troposphere, in *Composition, Chemistry, and Climate of the Atmosphere*, pp. 349–393. Van Nostrand Reinhold, New York (1995)
- Crutzen, P.J., Zimmermann, P.H.: The changing photochemistry of the troposphere. *Tellus B.* **43**(4), 136–151 (1991)
- Cvitas, T., Kezele, N., Klasinc, L., Lisac, I.: Tropospheric ozone measurements in Croatia. *Pure Appl. Chem.* **67**, 1450–1453 (1995)
- Delfino, R.J., Murphy-Moulton, A.M., Becklake, M.R.: Emergency room visits for respiratory illnesses among the elderly in Montreal: association with low level ozone exposure. *Environ. Res.* **76**(2), 67–77 (1998)
- Derwent, R.G., Simmonds, P.G., Seuring, S., Dimmer, C.: Observation and interpretation of the seasonal cycles in the surface concentrations of ozone and carbon monoxide at Mace head, Ireland from 1990 to 1994. *Atmos. Environ.* **32**(2), 145–157 (1998)
- Dickerson, R.R., Kondragunta, S., Stenichikov, G., Civerolo, K.L., Doddridge, B.G., Holben, B.N.: The impact of aerosols on solar ultraviolet radiation and photochemical smog. *Science*. **278**(5339), 827–830 (1997)
- Dominick, D., Juahir, H., Latif, M.T., Zain, S.M., Aris, A.Z.: Spatial assessment of air quality patterns in Malaysia using multivariate analysis. *Atmos. Environ.* **60**, 172–181 (2012)
- Dueñas, C., Fernández, M.C., Cañete, S., Carretero, J., Liger, E.: Assessment of ozone variations and meteorological effects in an urban area in the Mediterranean coast. *Sci. Total Environ.* **299**(1), 97–113 (2002)
- Finlayson-Pitts, B.J., Pitts Jr, J.N.: *Chemistry of the upper and lower atmosphere: theory, experiments, and applications*. Academic press (1999)
- Gao, Y., Arimoto, R., Duce, R.A., Lee, D.S., Zhou, M.Y.: Input of atmospheric trace elements and mineral matter to the Yellow Sea during the spring of a low-dust year. *Journal of Geophysical Research: Atmospheres*. **97**(D4), 3767–3777 (1992)
- Ghude, S.D., Jain, S.L., Arya, B.C., Kulkarni, P.S., Kumar, A., Ahmed, N.: Temporal and spatial variability of surface ozone at Delhi and Antarctica. *Int. J. Climatol.* **26**(15), 2227–2242 (2006)
- Ghude, S.D., Jain, S.L., Arya, B.C., Beig, G., Ahammed, Y.N., Kumar, A., Tyagi, B.: Ozone in ambient air at a tropical megacity, Delhi: characteristics, trends and cumulative ozone exposure indices. *J. Atmos. Chem.* **60**(3), 237–252 (2008)
- Gros, V., Poisson, N., Martin, D., Kanakidou, M., Bonsang, B.: Observations and modeling of the seasonal variation of surface ozone at Amsterdam Island: 1994–1996. *Journal of Geophysical Research: Atmospheres*. **103**(D21), 28103–28109 (1998)
- Hansen, J., Nazarenko, L., Ruedy, R., Sato, M., Willis, J., Del Genio, A., Koch, D., Lacis, A., Lo, K., Menon, S., Novakov, T.: Earth's energy imbalance: confirmation and implications. *Science*. **308**(5727), 1431–1435 (2005)
- Harris, J.M., Kahl, J.D.: A descriptive atmospheric transport climatology for the Mauna Loa observatory, using clustered trajectories. *Journal of Geophysical Research: Atmospheres*. **95**(D9), 13651–13667 (1990)
- Hopke, P.K.: Recent developments in receptor modeling. *J. Chemom.* **17**, 255–265 (2003)
- Iten, N., Selici, A.T.: Investigating the impacts of some meteorological parameters on air pollution in Balikesir, Turkey. *Environmental monitoring and assessment*. **140**(1–3), 267–277 (2008)
- Jacob, D.J.: Heterogeneous chemistry and tropospheric ozone. *Atmos. Environ.* **34**(12), 2131–2159 (2000)
- Jacobson, M.Z.: Strong radiative heating due to the mixing state of black carbon in atmospheric aerosols. *Nature*. **409**(6821), 695–697 (1998)
- Jain, S.L., Arya, B.C.: Surface ozone measurement over New Delhi. *Journal of Marine and Atmospheric research*. **2**(1), 22–25 (2001)
- Jain, S.L., Arya, B.C., Kumar, A., Ghude, S.D., Kulkarni, P.S.: Observational study of surface ozone at New Delhi. *India. International Journal of Remote Sensing*. **26**(16), 3515–3524 (2005)

- Jain, N., Bhatia, A., Pathak, H.: Emission of air pollutants from crop residue burning in India. *Aerosol Air Qual. Res.* **14**(1), 422–430 (2014)
- Jensen, E.J., Toon, O.: The potential impact of soot particles from aircraft exhaust on cirrus clouds. *Geophys. Res. Lett.* **24**(3), 249–252 (1997)
- Jobson, B.T., Wu, Z., Niki, H.: Seasonal trends of isoprene, C₂–C₅ alkanes and acetylene at a remote boreal site in Canada. *J. Geophys. Res.* **99**, 1589–1599 (1994)
- Kim, D.J., Pradhan, D., Chaudhury, G.R., Ahn, J.G., Lee, S.W.: Bioleaching of complex sulfides concentrate and correlation of leaching parameters using multivariate data analysis technique. *Mater. Trans.* **50**(9), 2318–2322 (2009)
- Kleinman, L., Lee, Y.N., Springston, S.R., Nunnermacker, L., Zhou, X., Brown, R., Hallock, K., Klotz, P., Leahy, D., Lee, J.H., Newman, L.: Ozone formation at a rural site in the southeastern United States. *Journal of Geophysical Research: Atmospheres.* **99**(D2), 3469–3482 (1994)
- Klonecki, A., Hess, P., Emmons, L., Smith, L., Orlando, J., Blake, D.: Seasonal changes in the transport of pollutants into the Arctic troposphere-model study. *J. Geophys. Res.* **108**, 8367 (2003)
- Li, G., Zhang, R., Fan, J., Tie, X.: Impacts of black carbon aerosol on photolysis and ozone. *Journal of Geophysical Research: Atmospheres* (1984–2012). **110**(D23), (2005)
- Li, M., Huang, X., Zhu, L., Li, J., Song, Y., Cai, X., Xie, S.: Analysis of the transport pathways and potential sources of PM₁₀ in Shanghai based on three methods. *Science of the Total Environment.* **414**, 525–534 (2012)
- Lin, W., Xu, X., Zhang, X., Tang, J.: Contributions of pollutants from North China plain to surface ozone at the Shangdianzi GAW Station. *Atmos. Chem. Phys.* **8**(19), 5889–5898 (2008)
- Logan, J.A.: Tropospheric ozone: seasonal behavior, trends, and anthropogenic influence. *Journal of Geophysical Research: Atmospheres.* **90**(D6), 10463–10482 (1985)
- Luria, M., Sievering, H.: Heterogeneous and homogeneous oxidation of SO₂ in the remote marine atmosphere. *Atmos. Environ. Part A.* **25**(8), 1489–1496 (1991)
- Ma, Z., Xu, J., Quan, W., Zhang, Z., Lin, W., Xu, X.: Significant increase of surface ozone at a rural site, north of eastern China. *Atmos. Chem. Phys.* **16**(6), 3969–3977 (2016)
- Mahapatra, P.S., Jena, J., Moharana, S., Srichandan, H., Das, T., Chaudhury, G.R., Das, S.N.: Surface ozone variation at Bhubaneswar and intra-corelation study with various parameters. *Journal of earth system science.* **121**(5), 1163–1175 (2012)
- Martins, D.K., Stauffer, R.M., Thompson, A.M., Knepp, T.N., Pippin, M.: Surface ozone at a coastal suburban site in 2009 and 2010: Relationships to chemical and meteorological processes. *Journal of Geophysical Research: Atmospheres* (1984–2012). **117**(D5), (2012)
- Mauderly, J.L., Chow, J.C.: Health effects of organic aerosols. *Inhal. Toxicol.* **20**(3), 257–288 (2008)
- Meng, Z., Dabdub, D., Seinfeld, J.H.: Chemical coupling between atmospheric ozone and particulate matter. *Science.* **277**(5322), 116–119 (1997)
- Mittal, M.L., Hess, P.G., Jain, S.L., Arya, B.C., Sharma, C.: Surface ozone in the Indian region. *Atmos. Environ.* **41**(31), 6572–6584 (2007)
- Monks, P.S.: A review of the observations and origins of the spring ozone maximum. *Atmos. Environ.* **34**(21), 3545–3561 (2000)
- Mosier, A.R., Duxbury, J.M., Freney, J.R., Heinemeyer, O., Minami, K., Johnson, D.E.: Mitigating agricultural emissions of methane. *Clim. Chang.* **40**(1), 39–80 (1998)
- Nair, P.R., Chand, D., Lal, S., Modh, K.S., Naja, M., Parameswaran, K., Ravindran, S., Venkataramani, S.: Temporal variations in surface ozone at Thumba (8.6 N, 77 E)-a tropical coastal site in India. *Atmospheric Environment.* **36**(4), 603–610 (2002)
- Naja, M., Lal, S.: Surface ozone and precursor gases at Gadanki (13.5 N, 79.2 E), a tropical rural site in India. *Journal of Geophysical Research: Atmospheres* (1984–2012). **107**(D14), ACH-8 (2002)
- Naja, M., Lal, S., Chand, D.: Diurnal and seasonal variabilities in surface ozone at a high altitude site Mt Abu (24.6 N, 72.7 E, 1680 m asl) in India. *Atmospheric Environment.* **37**(30), 4205–4215 (2003)
- Naja, M., Mallik, C., Sarangi, T., Sheel, V., Lal, S.: SO₂ measurements at a high altitude site in the central Himalayas: role of regional transport. *Atmos. Environ.* **99**, 392–402 (2014)
- Neue, H.U., Wassmann, R., Kludze, H.K., Bujun, W., Lantin, R.S.: Factors and processes controlling methane emissions from rice fields. *Nutr. Cycl. Agroecosyst.* **49**(1–3), 111–117 (1997)
- Nishanth, T.: Analysis of ground level O₃ and NO_x measured at Kannur, India. *Journal of Earth Science & Climatic Change.* **3**, (2012)
- Nishanth, T., Praseed, K.M., Kumar, M.S., Valsaraj, K.T.: Observational study of surface O₃, NO_x, CH₄ and Total NMHCs at Kannur, India. *Aerosol and Air Quality Research.* **14**(3), 1074–1088 (2014)
- Notario, A., Bravo, I., Adame, J.A., Diaz-de-Mera, Y., Aranda, A., Rodríguez, A., Rodríguez, D.: Behaviour and variability of local and regional oxidant levels (OX = O₃+ NO₂) measured in a polluted area in central-southern of Iberian peninsula. *Environ. Sci. Pollut. Res.* **20**(1), 188–200 (2013)

- Ojha, N., Naja, M., Singh, K.P., Sarangi, T., Kumar, R., Lal, S., Lawrence, M.G., Butler, T.M., Chandola, H.C.: Variabilities in ozone at a semi-urban site in the Indo-Gangetic Plain region: Association with the meteorology and regional processes. *Journal of Geophysical Research: Atmospheres*. **117**(D20), (2012)
- Oltmans, S.J., Levy, H.: Seasonal cycle of surface ozone over the western North Atlantic. *Nature*. **358**, 392–394 (1992)
- Oltmans, S.J., Levy, H., Harris, J.M., Merrill, J.T., Moody, J.L., Lathrop, J.A., Cuevas, E., Trainer, M., Prospero, J.M., Vömel, H., Johnson, B.J.: Summer and spring ozone profiles over the North Atlantic from ozonesonde measurements. *Journal of Geophysical Research: Atmospheres*. **101**(D22), 29179–29200 (1996)
- Özbay, B., Keskin, G.A., Doğruparmak, Ş.Ç., Ayberk, S.: Multivariate methods for ground-level ozone modeling. *Atmos. Res.* **102**(1), 57–65 (2011)
- Parrish, D.D.: Critical evaluation of US on-road vehicle emission inventories. *Atmos. Environ.* **40**(13), 2288–2300 (2006)
- Penner, J.E., Eddleman, H., Novakov, T.: Towards the development of a global inventory for black carbon emissions. *Atmos. Environ. Part A*. **27**(8), 1277–1295 (1993)
- Peshin, S.K., Sharma, A., Sharma, S.K., Mandal, T.K.: Seasonal variability of trace gases (O₃, NO, NO₂ and CO) and particulate matter (PM₁₀ and PM_{2.5}) over Delhi, India. *Vayu Mandal*. **40**(1–4), 61–73 (2014)
- Pochanart, P., Hirokawa, J., Kajii, Y., Akimoto, H., Nakao, M.: Influence of regional-scale anthropogenic activity in Northeast Asia on seasonal variations of surface ozone and carbon monoxide observed at Oki. Japan. *Journal of Geophysical Research: Atmospheres*. **104**(D3), 3621–3631 (1999)
- Pope III, C.A., Dockery, D.W.: Health effects of fine particulate air pollution: lines that connect. *J. Air Waste Manage. Assoc.* **56**(6), 709–742 (2006)
- Pope, C.A., Burnett, R.T., Thurston, G.D., Thun, M.J., Calle, E.E., Krewski, D., Godleski, J.J.: Cardiovascular mortality and long-term exposure to particulate air pollution: epidemiological evidence of general pathophysiological pathways of disease. *Circulation*. **109**(1), 71–77 (2004)
- Pope III, C.A., Ezzati, M., Dockery, D.W.: Fine-particulate air pollution and life expectancy in the United States. *N. Engl. J. Med.* **360**(4), 376–386 (2009)
- Pun, B.K., Seigneur, C., White, W.: Day-of-week behavior of atmospheric ozone in three US cities. *Journal of the Air & Waste Management Association*. **53**(7), 789–801 (2003)
- Purkait, N.N., De, S., Sen, S., Chakrabarty, D.K.: Surface ozone and its precursors at two sites in the northeast coast of India. *Indian J. Radio Space Phys.* **38**, 86–97 (2009)
- Ramanathan, V., Cicerone, R.J., Singh, H.B., Kiehl, J.T.: Trace gas trends and their potential role in climate change. *Journal of Geophysical Research: Atmospheres*. **90**(D3), 5547–5566 (1985)
- Reddy, R.R., Gopal, K.R., Reddy, L.S.S., Narasimulu, K., Kumar, K.R., Ahammed, Y.N., Reddy, C.K.: Measurements of surface ozone at semi-arid site Anantapur (14.62 N, 77.65 E, 331 m asl) in India. *Journal of Atmospheric Chemistry*. **59**(1), 47–59 (2008)
- Rodriguez, J.M., Ko, M.K., Sze, N.D.: Role of heterogeneous conversion of N₂O₅ on sulphate aerosols in global ozone losses. *Nature*. **352**, 134–137 (1991)
- Rückerl, R., Schneider, A., Breitner, S., Cyrys, J., Peters, A.: Health effects of particulate air pollution: a review of epidemiological evidence. *Inhal. Toxicol.* **23**(10), 555–592 (2011)
- Sacks, J.D., Stanek, L.W., Luben, T.J., Johns, D.O., Buckley, B.J., Brown, J.S., Ross, M.: Particulate matter-induced health effects: who is susceptible? *Environ. Health Perspect.* **119**(4), 446 (2011)
- Saini, R., Singh, P., Awasthi, B.B., Kumar, K., Taneja, A.: Ozone distributions and urban air quality during summer in Agra—a world heritage site. *Atmospheric Pollution Research*. **5**(4), 796–804 (2014)
- Saliba, M., Ellul, R., Camilleri, L., Güsten, H.: A 10-year study of background surface ozone concentrations on the island of Gozo in the Central Mediterranean. *J. Atmos. Chem.* **60**(2), 117–135 (2008)
- Schütz, L., Seibert, M.: Mineral aerosols and source identification. *J. Aerosol Sci.* **18**(1), 1–10 (1987)
- Schwartz, J.: Particulate air pollution and chronic respiratory disease. *Environ. Res.* **62**(1), 7–13 (1993)
- Sharma, P., Kuniyal, J.C., Chand, K., Guleria, R.P., Dhyani, P.P., Chauhan, C.: Surface ozone concentration and its behaviour with aerosols in the northwestern Himalaya. *India. Atmospheric Environment*. **71**, 44–53 (2013)
- Sharma, S.K., Mandal, T.K., Saxena, M., Sharma, A., Gautam, R.: Source apportionment of PM₁₀ by using positive matrix factorization at an urban site of Delhi. *India. Urban climate*. **10**, 656–670 (2014)
- Sharma, S.K., Sharma, A., Saxena, M., Choudhary, N., Masiwal, R., Mandal, T.K., Sharma, C.: Chemical characterization and source apportionment of aerosol at an urban area of Central Delhi. *India. Atmospheric Pollution Research*. **7**(1), 110–121 (2015)
- Sharma, A., Sharma, S.K., Rohtash, Mandal, T.K.: Influence of ozone precursors and particulate matter on the variation of surface ozone at an urban site of Delhi, India. *Sustainable Environment Research*. **26**(2), 76–83 (2016a)
- Sharma, S.K., Mandal, T.K., Jain, S., Saraswati, Sharma, A., Saxena, M.: Source apportionment of PM_{2.5} in Delhi, India using PMF model. *Bulletin of Environmental Contamination and Toxicology*. **97**, 286–293 (2016b)

- Stachelin, J., Harris, N.R.P., Appenzeller, C., Eberhard, J.: Ozone trends: A review. *Rev. Geophys.* **39**(2), 231–290 (2001)
- Statheropoulos, M., Vassiliadis, N., Pappa, A.: Principal component and canonical correlation analysis for examining air pollution and meteorological data. *Atmos. Environ.* **32**(6), 1087–1095 (1998)
- Thompson, A.M.: The oxidizing capacity of the Earth's atmosphere: probable past and future changes. *Science*. **256**(5060), 1157–1165 (1992)
- Tilton, B.E.: Health effects of tropospheric ozone. *Environ. Sci. Technol.* **23**(3), 257–263 (1989)
- Toh, Y.Y., Lim, S.F., Von Glasow, R.: The influence of meteorological factors and biomass burning on surface ozone concentrations at Tanah Rata, Malaysia. *Atmospheric Environment*. **70**, 435–446 (2013)
- Tu, J., Xia, Z.G., Wang, H., Li, W.: Temporal variations in surface ozone and its precursors and meteorological effects at an urban site in China. *Atmos. Res.* **85**(3), 310–337 (2007)
- Varotsos, C.A., Efstathiou, M.N., Kondratyev, K.Y.: Long-term variation in surface ozone and its precursors in Athens, Greece: a forecasting tool. *Environmental science and pollution research international*. **10**(1), 19–23 (2002)
- Varotsos, C.A., Ondov, J.M., Efstathiou, M.N., Cracknell, A.P.: The local and regional atmospheric oxidants at Athens (Greece). *Environ. Sci. Pollut. Res.* **21**(6), 4430–4440 (2014)
- Varshney, C.K., Aggarwal, M.: Ozone pollution in the urban atmosphere of Delhi. *Atmospheric Environment. Part B. Urban Atmosphere*. **26**(3), 291–294 (1992)
- Vellingiri, K., Kim, K.H., Jeon, J.Y., Brown, R.J., Jung, M.C.: Changes in NO_x and O₃ concentrations over a decade at a central urban area of Seoul, Korea. *Atmospheric Environment*. **112**, 116–125 (2015)
- Wang, Y.Q., Zhang, X.Y., Draxler, R.R.: TrajStat: GIS-based software that uses various trajectory statistical analysis methods to identify potential sources from long-term air pollution measurement data. *Environmental Modelling & Software*. **24**(8), 938–939 (2009)
- Wayne, R.P., Barnes, I., Biggs, P., Burrows, J.P., Canosa-Mas, C.E., Hjorth, J., Le Bras, G., Moortgat, G.K., Perner, D., Poulet, G., Restelli, G.: The nitrate radical: physics, chemistry, and the atmosphere. *Atmos. Environ. Part A*. **25**(1), 1–203 (1991)
- Weschler, C.J.: Ozone's impact on public health: contributions from indoor exposures to ozone and products of ozone-initiated chemistry. *Environmental health perspectives*. 1489–1496 (2006)
- Wesely, M.L., Hicks, B.B.: A review of the current status of knowledge on dry deposition. *Atmos. Environ.* **34**(12), 2261–2282 (2000)
- Yerramsetti, V.S., Gauravarapu Navlur, N., Rapolu, V., Dhulipala, N.S.K., Sinha, P.R., Srinivasan, S., Anupaju, G.R.: Role of nitrogen oxides, black carbon, and meteorological parameters on the variation of surface ozone levels at a tropical urban site—Hyderabad, India. *Clean–Soil, Air, Water*. **41**(3), 215–225 (2013)
- Yong, A.G., Pearce, S.: A beginner's guide to factor analysis: focusing on exploratory factor analysis. *Tutorials in Quantitative Methods for Psychology*. **9**(2), 79–94 (2013)
- Zhang, Y., Sunwoo, Y., Kotamarthi, V., Carmichael, G.R.: Photochemical oxidant processes in the presence of dust: an evaluation of the impact of dust on particulate nitrate and ozone formation. *J. Appl. Meteorol.* **33**(7), 813–824 (1994)
- Zhang, H., Wang, Y., Hu, J., Ying, Q., Hu, X.M.: Relationships between meteorological parameters and criteria air pollutants in three megacities in China. *Environ. Res.* **140**, 242–254 (2015)